The impact of magnetic dilution on magnetic order in $MnPS_3$

2000 J. Phys.: Condens. Matter 12 4233

(http://iopscience.iop.org/0953-8984/12/18/308)

J. Phys.: Condens. Matter **12** (2000) 4233–4242. Printed in the UK PII: S0953-8984(00)10459-X

The impact of magnetic dilution on magnetic order in $MnPS_3$

D J Goossens†§, A J Studer‡, S J Kennedy‡ and T J Hicks†

† Department of Physics, Monash University, Clayton 3168, Australia

‡ Neutron Scattering Group, Physics Division, Australian Nuclear Science and Technology Organisation, Menai 2234, Australia

E-mail: goossens@rsc.anu.edu.au

Received 20 December 1999

Abstract. $MnPS_3$ is a layered honeycomb lattice antiferromagnet with the spins aligned perpendicular to the layers at low temperature. Structurally it is monoclinic, with an unusual combination of magnetic and crystallographic symmetries, and so offers a rare insight into the behaviour of low-dimensional magnetism. Here the effect of magnetic dilution by Zn substitution on the magnetic structure is explored using neutron diffraction and magnetometry. The composition dependencies of T_N and the spin flop field are found. The critical concentration for long-range order is estimated to be 45% Mn. The first neighbour exchange is found to be independent of composition. It appears that dilution induces a moment component in the plane, and gives rise to a complex phase diagram in which a reordering temperature is apparent.

1. Introduction

Manganese thiophosphate, $MnPS_3$, is a layered, quasi-two-dimensional (2-d) Heisenberg antiferromagnet. In the ordered regime, a small anisotropy aligns the moments normal to the layer planes. This normal is defined as the Cartesian z direction. The Néel temperature, T_N, is 78 K at low fields ($H_z < 40$ kOe, where H_z is a magnetic field applied along z) [1]. $MnPS_3$ has a monoclinic structure with space group $C_{2/m}$. Lattice parameters are $a = 6.077$ Å, $b = 10.524$ Å, $c = 6.796$ Å and $\beta = 107.35^\circ$ [2]. Hence, the c axis is not parallel with the z direction. In the layers, manganese atoms form a honeycomb lattice. Every manganese is neighboured by three manganese atoms and three P_2 pairs [2]. Each such layer lies between a pair of sulphur layers. These triple structures are joined to each other by Van der Waals forces between adjacent sulphur layers. The distance between manganese layers and the complex exchange path give rise to the 2-d magnetism exhibited by $MnPS_3$.

The Mn^{2+} ions interact antiferromagnetically ($J_1/k_B \sim 8$–10 K) [3–6] with their three intraplanar nearest neighbours, and are ordered ferromagnetically with their interplanar nearest neighbours [1] (see figure 1). The current estimate of the ratio of interplanar (J') to intraplanar first neighbour exchange (J_1) is of the order of $1/400$ [6]. The interplanar exchange should be thought of as an effective exchange, as the complex exchange path between layers may mean that nearest interplanar neighbours do not interact directly. The distance between interplanar nearest neighbours is similar to that between in-plane second and third neighbours while the ratio of exchange interactions is about $1/100$, and the exchange couplings, J_2 and J_3, between the in-plane neighbours have been shown to be antiferromagnetic [6].

§ Corresponding author. Tel: +61 2 6249 3579, Fax: +61 2 6249 0750. Current address: Research School of Chemistry, Australian National University, Canberra 0200, Australia.

0953-8984/00/184233+10$30.00

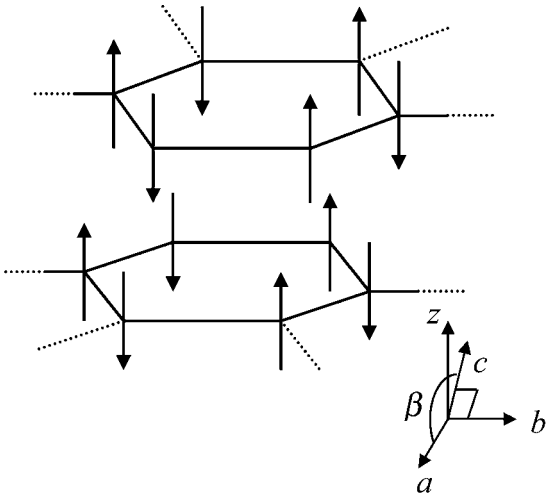

Figure 1. The magnetic structure of $MnPS_3$, with arrows representing direction of magnetic moments on Mn^{2+} ions and the directions a, b, c and z defined.

The aim of this work is to explore the effect of magnetic dilution on the ordering. To do this, neutron diffraction scans and SQUID magnetometer experiments were performed at temperatures above and below T_N on samples of $Mn_xZn_{1-x}PS_3$ where $x = 0.55$ to 1.

2. Experimental details

The magnetometer experiments were performed in the Department of Physics at Monash University using a Quantum Design MPMS-7 SQUID magnetometer, capable of making measurements over a temperature range of 2–350 K and an applied field range of 0–70 kOe. The magnetic field could be applied along the spin direction or perpendicular to it. Single crystals of $Mn_xZn_{1-x}PS_3$ were used for these experiments. The neutron diffraction work was performed at the HIFAR reactor at Lucas Heights in Sydney using the medium resolution powder diffractometer (MRPD) [7].

Samples of $Mn_xZn_{1-x}PS_3$ were grown using a vapour transport technique [2, 5]. Good single crystals were separated out for use in magnetometry. The remaining mass of crystals was ground up and divided into two amounts with masses in the ratio 2:1. These amounts of powder were then uniaxially pressed and mounted orthogonally such that the axis of the smaller pellet lay in the scattering plane of the diffractometer. This sample geometry was chosen to minimize preferred orientation effects. Low temperature scans were made using a closed cycle helium refrigerator. Scans were done with the sample angle ω varying from 0 to 180° in steps of 10° and then averaged to combat plane preferred orientation. Further allowance could be made during the fitting.

The diffraction patterns were analysed using the Rietveld method as implemented by the LHPM program developed by Howard and Hunter [8] and the FullProf program, developed by Rodriguez-Carvajal [9]. The latter program was used to solve for the magnetic structures because it contains routines for performing magnetic structure refinements as well as atomic structure refinements. LHPM was useful in analysing room temperature patterns and in establishing structural parameters.

Despite the difficulties introduced by the presence of 2-d Bragg peak shapes [10, 11], the data could be analysed using the Rietveld method if suitable uncertainties were attached to the results. Manipulating the function describing the instrument resolution could make some allowance for the unusual line shape, as could using the peak asymmetry parameters incorporated into the Rietveld programs. While fitting individual peaks would have allowed a more correct 2-d line shape to be used, it was necessary to reliably separate the effect of preferred orientation (which was different for each sample, and which was present at high temperatures due to the persistence of magnetic critical fluctuations [6]) from that of the changing spin structure. This required a global fit, and hence this is the technique used. Due to these compromises, the fraction of magnetic moment along each crystallographic direction could not be reliably determined, but it was possible to determine, with some reliability, the fraction of magnetic moment in the *ab* plane and in the *z* direction.

3. Results from neutron scattering

The magnetic structure factor for neutron scattering from the spin arrangement shown in figure 1 with a $C_{2/m}$ space group can be written as

$$F_M \approx \mu_\perp 4i \sin\left(\frac{2\pi k}{3}\right) \tag{1}$$

where k is a Miller index and $\mu_\perp$ is the component of the magnetic moment perpendicular to the scattering vector. Therefore Bragg peaks for which $k = 3n$ (where n is an integer) have zero magnetic intensity. This rule was found to be obeyed by all samples, meaning that the ordering remained antiferromagnetic regardless of composition, and no ferromagnetic component was induced. This was a valuable result, as it gave a useful starting point for the Rietveld analysis.

Rietveld fitting was performed on all neutron diffraction data sets. Using TEM, XRD and these neutron diffraction results, samples were found to be of the correct structure, and of single phase. Phase separation was found from this study to be absent from the $Mn_xZn_{1-x}PS_3$ series, which was a useful result and in general agreement with Chandrasekharan and Vasudevan [3] who believed the Zn to substitute randomly onto the Mn sites.

The result obtained from fitting the high-temperature data was a measure of the preferred orientation in the samples. The preferred orientation axis was defined as the c axis due to the platelet nature of the crystals. Preferred orientation was found to be high (March parameter $G1 > 3$), with the samples behaving as if they had a strongly platelet-like character.

After fitting the high-temperature diffraction pattern, the magnetic phase was added to the Rietveld refinement and the fits were performed for the low-temperature data. The 2-d line-shapes that gave rise to large uncertainties in the results can be seen in the (020)/(110) in figure 2. Interestingly, the $k \neq 3n$ peaks have considerable widths and 2-d line-shapes even at very low temperature, while the $k = 3n$ peaks (the non-magnetic peaks) have widths which can be wholly attributed to instrument resolution and show no sign of 2-d line-shapes. This was common to all compositions. This suggests that some magnetic correlations lengths in at least some of the crystallites in each sample are finite—calculation from the Scherrer equation suggests lengths of the order of hundreds of Angstroms—while the atomic correlations are effectively infinite. This may suggest the formation of antiferromagnetic domains. This is supported by single-crystal diffraction experiments at low temperatures, which show a component of the magnetic scattering which is rod like with a short correlation length along the z direction and a rather longer correlation in the plane [12].

Figure 3 shows the average magnitude of the magnetic moment on the Mn atoms as a function of composition at 3.5 K. This is found to be $4.5 \pm 0.2\ \mu_B$ in the pure material, in

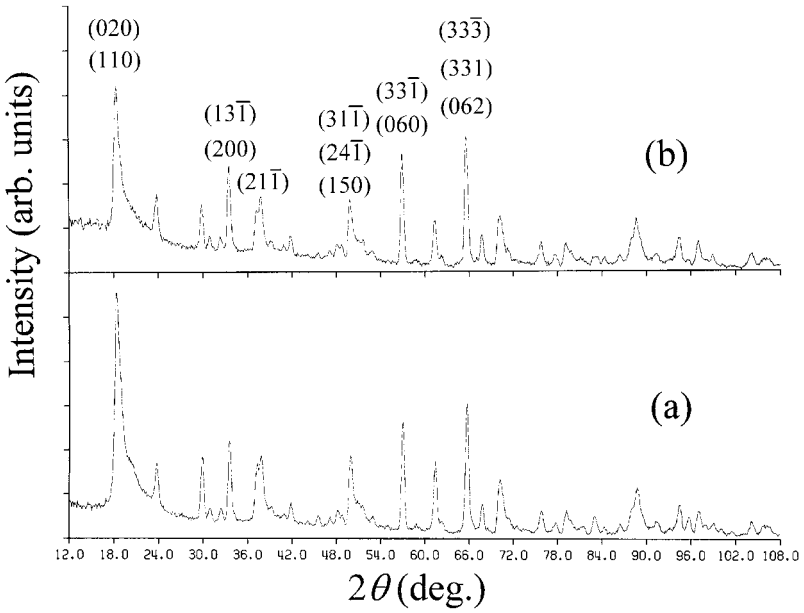

Figure 2. Powder diffraction patterns with $\lambda = 1.67$ Å for $Mn_{0.79}Zn_{0.21}PS_3$ (a) at 3.5 K (b) at 200 K, various reflections noted. The asymmetry of the magnetic features made up of the (020) and (110) reflections and made up of the (31$\bar{1}$), (24$\bar{1}$) and (150) reflections becomes apparent when compared with the similarly intense (33$\bar{1}$) and (060) feature and the (33$\bar{3}$), (331) and (062) feature—extra intensity on the high angle side is apparent. This asymmetry is due to scattering from the 2-d magnetic structure. Note that it is not present in peaks for which $k = 3n$, which are non-magnetic peaks.

agreement with a value of $4.1 \pm 0.3\ \mu_B$ found using neutron diffraction from a stack of platelet crystals in [1]. As $2S = 5$, the zero point spin defect is about 10%—a reasonable figure, given that Mn^{2+} is a high spin ion with low magnetic coordination but, as noted below, substantial second and third nearest neighbour interactions [6]. The $x = 0.65$ data, which was collected at 15 K, has been corrected using the staggered magnetization versus temperature curve for $S = 5/2$, as Mn^{2+} in $MnPS_3$ has been shown to obey this law well at such temperatures [1]. Figure 3 shows that the magnitude decreases as dilution increases. However, this does not entirely reflect a reduction in the actual moment per atom. The manganese occupation measures the number of manganese atoms present, whereas the magnetic intensity measured is due to atoms in the long range ordered (LRO) cluster. However, atoms which have lower coordinations will have larger zero point spin defects [13], while atoms which are not connected to the LRO cluster will not contribute at all to the magnetic Bragg intensity. Hence, the values in figure 3 do not give the actual average magnetic moment on the atoms in the infinite cluster, but can be thought of as lower bounds, with 4.5 μ_B as the upper bound. If it is assumed that the magnitude of the moments on individual atoms is 4.5 μ_B, estimates of lower bounds of the fraction of ion sites (Mn or Zn) connected to the infinite magnetic long range ordered cluster can be gained. These prove to be 0.35, 0.53, 0.76 and 0.83 for the $x = 0.55$, 0.65, 0.79 and 0.85 samples respectively. As disorder increases, it becomes likely that the magnetic structure will deviate randomly from collinearity, so that the components of some moments will cancel with those of others, reducing the average moment measured. This is a difficult factor for which to allow, but it is another reason why the fractions quoted above are lower bounds.

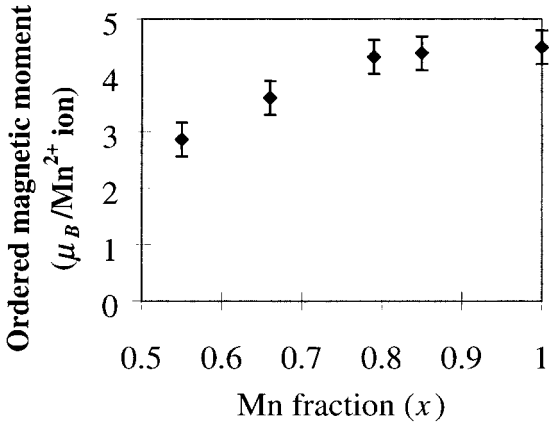

Figure 3. Ordered magnetic moment magnitude per manganese versus manganese content at 3.5 K.

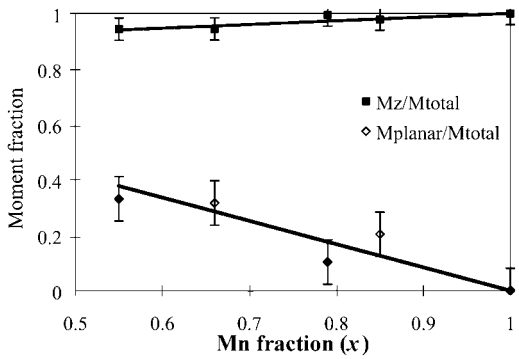

Figure 4. Fractional magnetic moment component along z (■) and in the ab plane (♦) as a function of manganese content at 3.5 K. Lines are guides to the eyes.

Figure 4 shows the dependence of the staggered moment component along z and in the ab plane on composition, as derived from Rietveld results. Components are expressed as fractions of the moment magnitudes in figure 3.

The moments remain predominantly directed (anti)parallel with the z direction, although the tilt is 18° at $x = 0.55$. An antiferromagnetic in-plane component arises, and increases as the sample becomes more magnetically dilute to become about $1/3$ as large as that along the z direction when $x = 0.55$. As noted, the direction of the component cannot be ascertained with any certainty from these data. The anisotropy in $MnPS_3$ is mostly dipolar in origin [4, 15]. When the system is diluted, the dipolar field at each site will be unique. Due to the monoclinic structure the local moment components along a will not average to zero. Absence of the closest Mn atom in either the plane above or below a given atom will produce a field component along a (figure 5). This is because the local dipole field for a completely full cation lattice is along the z direction so any absence will produce a canting of the moment directly above or below it. The direction of the canting will depend on the sublattice which the site belongs to so that an average staggered moment is set up perpendicular to the z direction along the a axis. It must be stressed that these are *average* effects, and that because of the randomness the actual direction of a moment on a given site cannot be known.

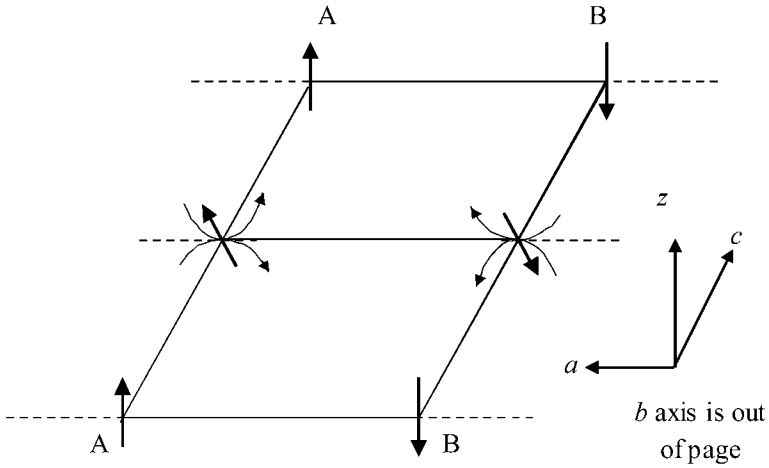

Figure 5. Schematic view of the $MnPS_3$ spin structure, looking down the b axis. In the fully occupied lattice, the total dipole field is in the z direction. The fields at the central atoms due to those directly above and below are shown as curved arrows. If either of the A atoms is removed, its dipole field contribution is lost and the Mn spin in the layer between cants as shown. If either of the B atoms is removed a similar but opposite canting results. This gives a net *staggered* moment along the a axis.

It can be noted that the critical concentration in a 2-d honeycomb lattice with first neighbour interaction only is $x = 0.7$ [14] whereas here a staggered moment has been observed at $x = 0.55$. This supports magnetometer measurements in [5], which found order to persist to these Mn concentrations, and agrees with [6], in which it was observed that first neighbour interactions alone are insufficient to fit the spin wave spectrum of $MnPS_3$.

4. Results from SQUID magnetometry

Using magnetometry, Chandrasekharan and Vasudevan [3] closely examined the $Mn_xZn_{1-x}PS_3$ system for $x = 0.05$ to 1. They found the first neighbour exchange to be $J_1/k_B = -8.1$ K, independent of x, and that the Curie–Weiss temperature, Θ, decreased linearly with x from a value of -160 K when $x = 1$. Further, they saw no evidence of order for $x < 0.7$.

Results from [5] combined with further measurements allow the ordering temperature to be plotted as a function of composition. This can be seen in figure 6. The curve is not linear. At approximately $x = 0.7$—the nearest neighbour percolation threshold—the gradient changes substantially. The two straight lines on the figure are linear fits above and below this change in gradient. Both fits are very good in their respective regions, with the gradient of the upper fit being 1.35, which is quite reasonable in the light of calculations of the expected dependence of T_N on x in a 2-d magnetic system [19], although no results for a honeycomb lattice with $S = 5/2$ were available for a direct comparison. The lower fit extrapolates to a critical concentration, p_c, of 0.45, although this is an approximation as no data points are very close to this value. Similar results could be gained from the spin flop field, H_{sf}, where extrapolation gives $p_c = 0.48$.

These results and those in section 3 show that order does exists when $x < 0.7$. This confirms the significance of interactions other than the nearest neighbour, which agrees with results presented in [6]. As [3] does not go to temperatures below 30 K, the disagreement

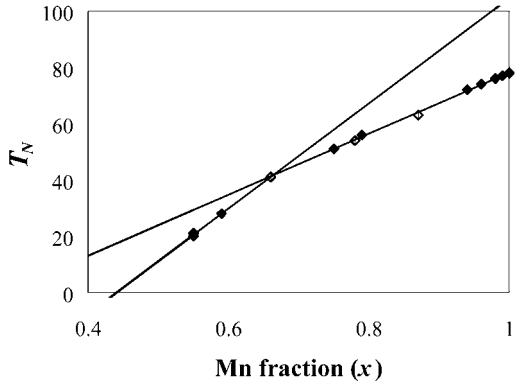

Figure 6. T_N as a function of composition. ♦ indicates measured data, the lines are linear fits to point above and below $x = 0.7$.

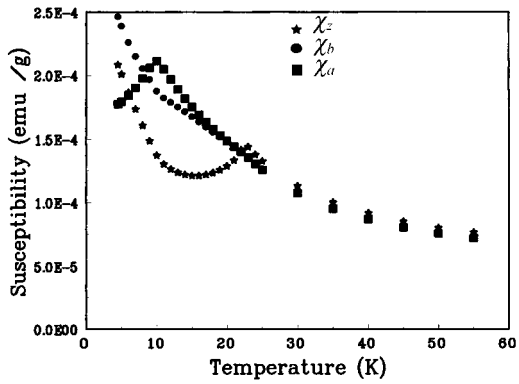

Figure 7. The magnetic susceptibilities for a sample of $Mn_{0.55}Zn_{0.45}PS_3$ measured along z, a and b (denoted χ_z, χ_a and χ_b respectively) at 100 Oe.

between results presented there and here is not large. In other aspects, the work here agrees with that in [3]. Fitting a high temperature series expansion [3, 16] to SQUID magnetometer data showed that the susceptibility could indeed be fitted by $J_1/k_B = -8.1$ K if a Curie term was added at large dilutions to allow for the population of spins which are not connected to the long range ordered cluster. Also, fitting a Curie–Weiss law to the high temperature data gave Curie–Weiss temperatures which did indeed fall linearly with x. However, Θ was found to be -300 K at $x = 1$, a large discrepancy which cannot be easily accounted for, but which was found to be consistent over different samples and crystal growths. This problem may be related to the unreliability of mean field theory when applied to low dimensional systems. It can be noted that Θ has also been found to be -230 K [4], -217 [17] and -315 K [18], so this quantity has not yet been completely established.

Figure 7 shows the DC susceptibilities at 100 Oe for a sample of $Mn_{0.55}Zn_{0.45}PS_3$ measured along z, a and b (denoted χ_z, χ_a and χ_b respectively). The directions of a and b were determined using x-ray Laue photographs and agreed with the directions suggested by optical microscopy. χ_z shows an apparent phase transition at about 20 K, although at very low temperatures χ_z is quite large, due partly to the existence of paramagnetic spins and also, from the results in section 3, due to the existence of a spin component in the plane, and hence perpendicular to

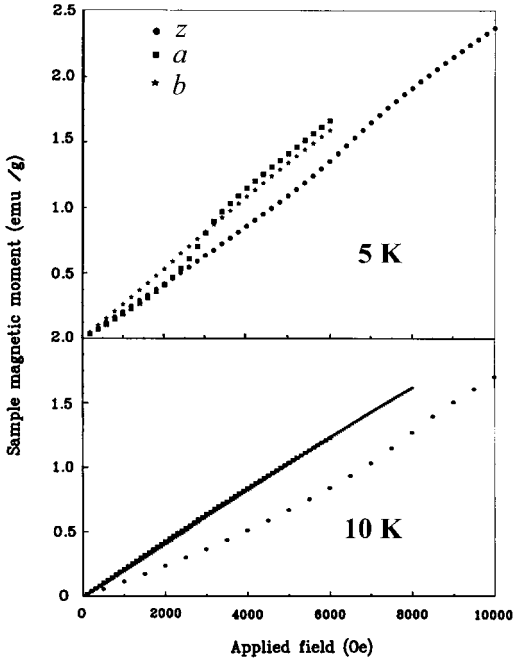

Figure 8. Magnetic moment as a function of applied field magnitude and direction for a sample of $Mn_{0.55}Zn_{0.45}PS_3$ at 5 K and 10 K. Curves are denoted a, b and z, indicating that the magnetic field was applied parallel with that direction. The absence of the in-plane spin flop at 10 K can be seen.

the field direction. Importantly, the two in-plane susceptibilities, χ_a and χ_b, are no longer identical. The gradient of χ_a shows a discontinuity at about 9 K, while χ_b also shows a change in slope. With χ_a rising to a cusp and χ_b falling to the discontinuity, these two susceptibilities are suggestive of parallel and perpendicular antiferromagnet susceptibilities respectively. This suggests that the in-plane spin component found in section 3 is along a, which agrees with a dipolar mechanism for the anisotropy, a good sign of consistency. Only at temperatures above 20 K do all three susceptibilities coincide, so this must be the ordering temperature.

If there is a spin component along a then applying an increasing field along a should result in a spin–flop transition. This was observed at 5 K, and is plotted in figure 8, with the three curves denoted z, a and b. The spin flop with the field along z can be seen at close to 6000 Oe in the 5 K experiment ($T = 5$ K), as expected [5]. The curve labelled a also shows a strong change in gradient, although at about 3000 Oe. No such change can be observed in curve b. Hence, it can be concluded that the dilution-induced spin component is perpendicular to the b direction, and therefore lies along the a direction—the same direction as the monoclinic distortion. Thus, when dilution adds a random component to the dipolar field experienced by each moment, the crystallographic symmetry means that along the a axis these components do not cancel out, resulting in the average moment being canted away from the z direction and into the a direction.

An equivalent set of experiments was done at 10 K to gain insight into the state of the system between 9 K and 20 K—above the cusp in χ_a but below T_N. These results are plotted in the lower half of figure 8, and show that an ordered z spin component still exists, but that there is now no ordered in-plane spin component. As the dipolar interaction falls with temperature, it is reasonable that the induced spin component will fall. It appears that at 9 K, the in-plane

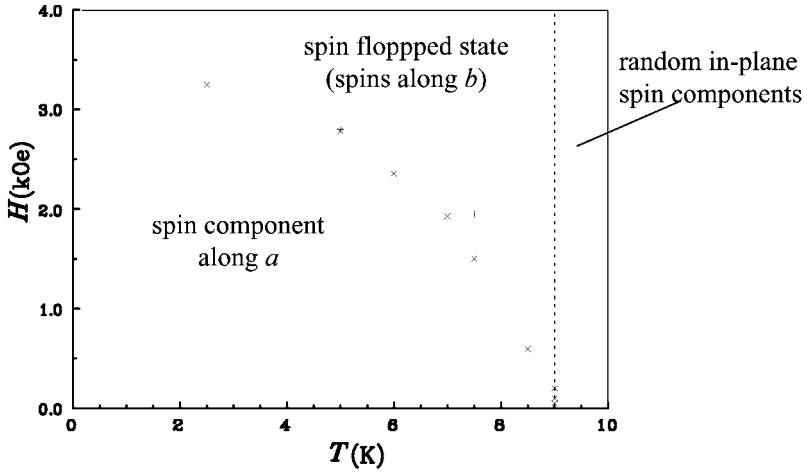

Figure 9. The magnetic phase diagram for the in-plane spin component in $Mn_{0.55}Zn_{0.45}PS_3$. Measurements are taken against temperature at constant field (+) and against field at constant temperature (×). The dashed line indicates a suggested reordering phase boundary.

spin components become disordered, and the system changes into a state with ordered spin components in the z direction but with any moments along a and b averaging to zero. Hence, the cusp in χ_a appears to be a reordering temperature. The T/H_z magnetic phase diagram for $Mn_{0.55}Zn_{0.45}PS_3$ is shown in [5]. Figure 9 here shows a suggested T/H_a phase diagram. The enclosed region is where the in-plane spin component is along a. The spin flop phase is where this in-plane component flops to be along the b direction. A hypothesized boundary has been inserted to indicate the reordering temperature. At 20 K, the transition to full paramagnetism takes place.

The in-plane disorder that exists between 10 and 20 K is probably dynamic, if thermally induced; but that cannot be ascertained from these data.

5. Conclusions

It was found that good quality single crystal samples of $Mn_xZn_{1-x}PS_3$ could be grown using vapour transport. Neutron diffraction showed that pure $MnPS_3$, even at very low temperature, shows evidence of finite magnetic correlation lengths, possibly reflecting a magnetic domain structure. The magnetic moment on the Mn^{2+} ion was found to be $4.5\pm0.2\ \mu_B$ in the pure material. Diffraction also showed that magnetic dilution induces an in-plane moment component which, when 45% of the magnetic sites are vacant, results on average in approximately 30% of the magnetic moment lying in the plane. This component is directed along the a direction. This was determined from SQUID magnetometry results, especially by noting the magnetic field direction dependence of the spin flop phase transition. SQUID results also suggested that, in $Mn_{0.55}Zn_{0.45}PS_3$, the in-plane component becomes ordered at temperatures smaller than 9 K, while the Néel temperature for this composition is close to 20 K. This behaviour appears consistent with a dipolar mechanism for the anisotropy. The first neighbour exchange appears to be independent of composition, while the existence of order when fewer than 70% of the magnetic sites are occupied indicates that first neighbour interactions do not fully explain the behaviour of $Mn_xZn_{1-x}PS_3$. The critical composition was estimated to be at $x = 0.46 \pm 0.03$.

These results show that the combination of the low symmetry of $MnPS_3$ with magnetic dilution results in interesting and unusual ordering phenomena.

Acknowledgments

We would like to thank Mr Roman Liebach for materials preparation assistance, Mr Rod Mackie for x-ray assistance and Dr Andrew Wildes for helpful discussions. The financial assistance of the Australian Research Council and the Australian Institute of Nuclear Science and Engineering (AINSE) is gratefully acknowledged. DJG was the recipient of a Monash Postgraduate Publications Award, an Australian Postgraduate Award and an AINSE supplement.

References

[1] Kurosawa K, Saito S and Tamaguchi Y 1983 *J. Phys. Soc. Japan* **52** 3919–26
[2] Ouvrard G, Brec R and Rouxel J 1985 *Mat. Res. Bull.* **20** 1181–9
[3] Chandrasekharan N and Vasudevan S 1996 *Phys. Rev.* B **54** 14 903–6
[4] Okuda K, Kurosawa K, Saito S, Honda M, Yu Z and Date M 1986 *J. Phys. Soc. Japan* **55** 4456–63
[5] Goossens D J and Hicks T J 1998 *J. Phys.: Condens. Matter* **10** 7643–52
[6] Wildes A R, Roessli B, Lebech B and Godfrey K W 1998 *J. Phys.: Condens. Matter* **10** 6417–28
[7] Kennedy S J 1995 *Adv. X-ray Anal.* **38** 35–46
[8] Howard C J and Hunter B A 1996 *A Computer Program for Rietveld Analysis of X-ray and Neutron Powder Diffraction Patterns* Australian Nuclear Science and Technology Organisation, Lucas Heights Research Laboratories, Sydney
[9] Rodriguez-Carvajal J 1993 *Physica* B **192** 55–69
[10] Schildberg H P and Lauter H J 1989 *Surf. Sci.* **208** 507–32
[11] Warren B E 1941 *Phys. Rev.* **59** 693–8
[12] Wildes A R 1999 Private communication
[13] Lines M E 1970 *J. Phys. Chem. Solids* **31** 101–16
[14] Shante V K S and Kirkpatrick S 1971 *Adv. Phys.* **20** 325–57
[15] Joy P A and Vasudevan S 1992 *Phys. Rev.* B **46** 5425–33
[16] Morgan D J and Rushbrooke G S 1961 *Mol. Phys.* **4** 291–303
[17] Le Flem G, Brec R, Ouvrard G, Louisy A and Segransan P 1982 *J. Phys. Chem. Solids* **43** 455–61
[18] Wildes A R 1994 *PhD Thesis* Monash University
[19] Rushbrooke G S, Muse R A, Stephenson R L and Pirnie K 1972 *J. Phys. C: Solid State Phys.* **5** 3371–86